Repetitive concussive and subconcussive injury in a human tau mouse model results in chronic cognitive dysfunction and disruption of white matter tracts, but not tau pathology

Mihika Gangolli, Joseph Benetatos, Thomas J. Esparza, Emeka M. Fountain, Shamilka Seneviratne, David L. Brody

Supplementary Information

Supplementary Figures

Supplementary Tables

Supplementary References

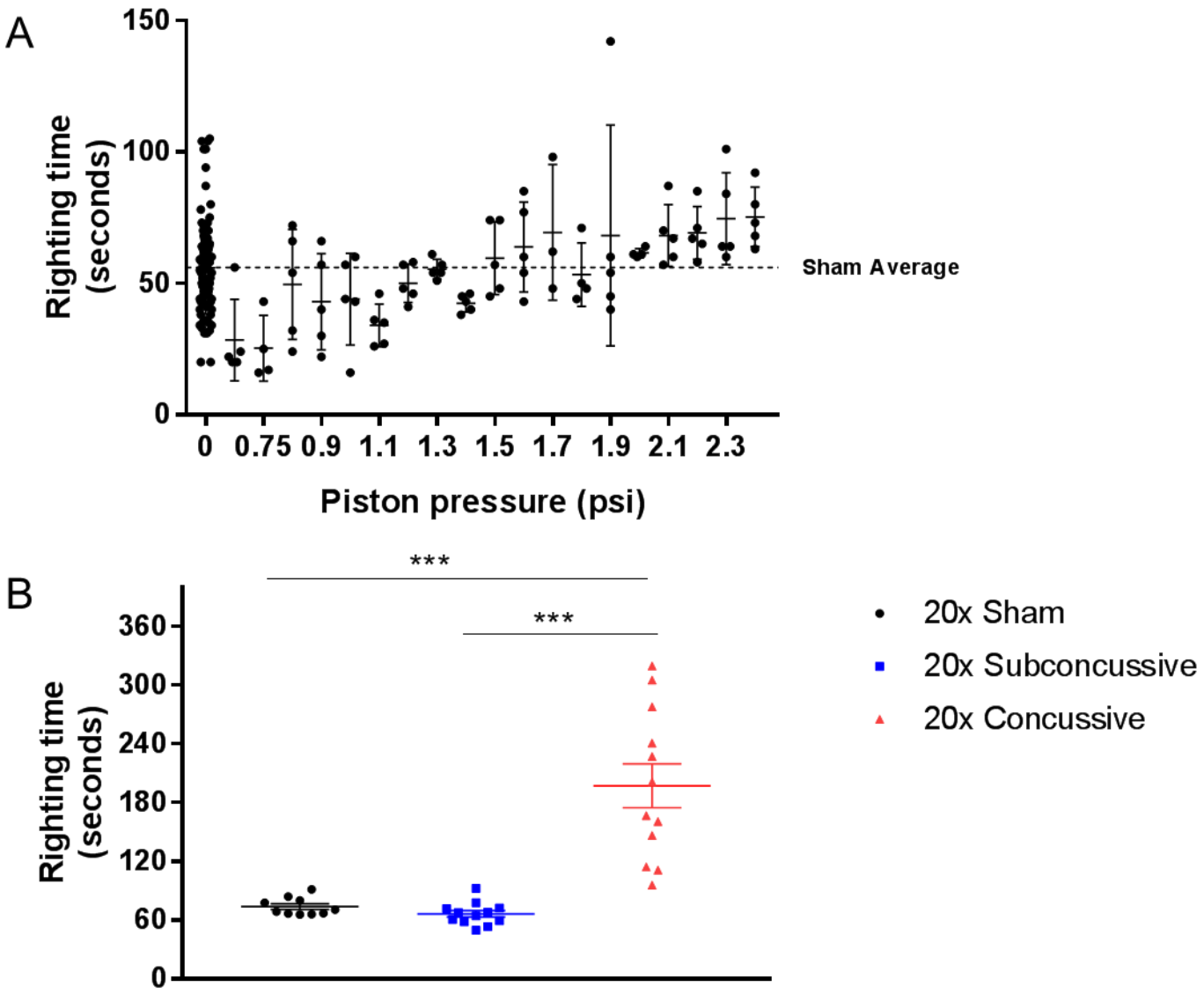

Supplemental Figure 1. Determination of impact thresholds. A. Wild type mice were randomly assigned to receive a single impact with the CHIMERA piston pressure set to a value between 0 (sham) and 2.4 psi. Latency to righting reflex (righting time) was measured following impact for each animal. Mice in groups receiving an impact of 2.0 psi or higher had mean righting times greater than the sham average (56 seconds), with standard deviations that did not overlap with the sham average righting time. **B.** In a separate experiment, mice (n = 10-12 per group) received daily concussive (3.1 psi) or subconcussive (2.0 psi) injuries for twenty consecutive days. Mice in the 20x concussive group had increased righting times averaged over the course of the twenty days relative to shams ($p = 0.000126$) and animals in the 20x subconcussive group ($p = 0.000125$). There was no difference between sham animals and 20x subconcussive animals.

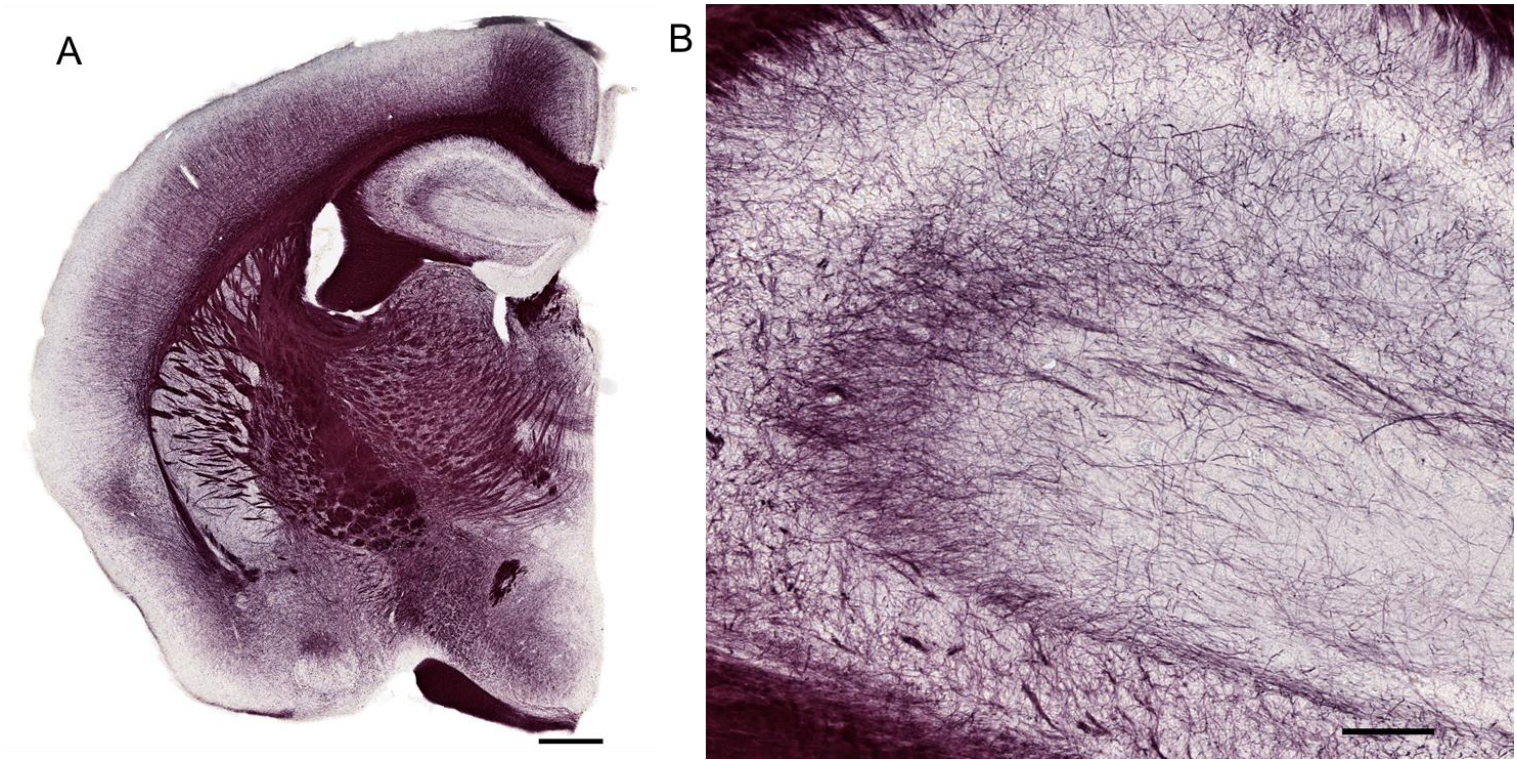

Supplemental Figure 2. Myelin Black Gold II staining. A. 50 µm free floating sections were incubated in Black Gold II solution for 8-12 minutes. Scale bar = 500 microns. **B.** Staining was completed once the mossy fibers of the hippocampus were stained. Scale bar = 100 microns.

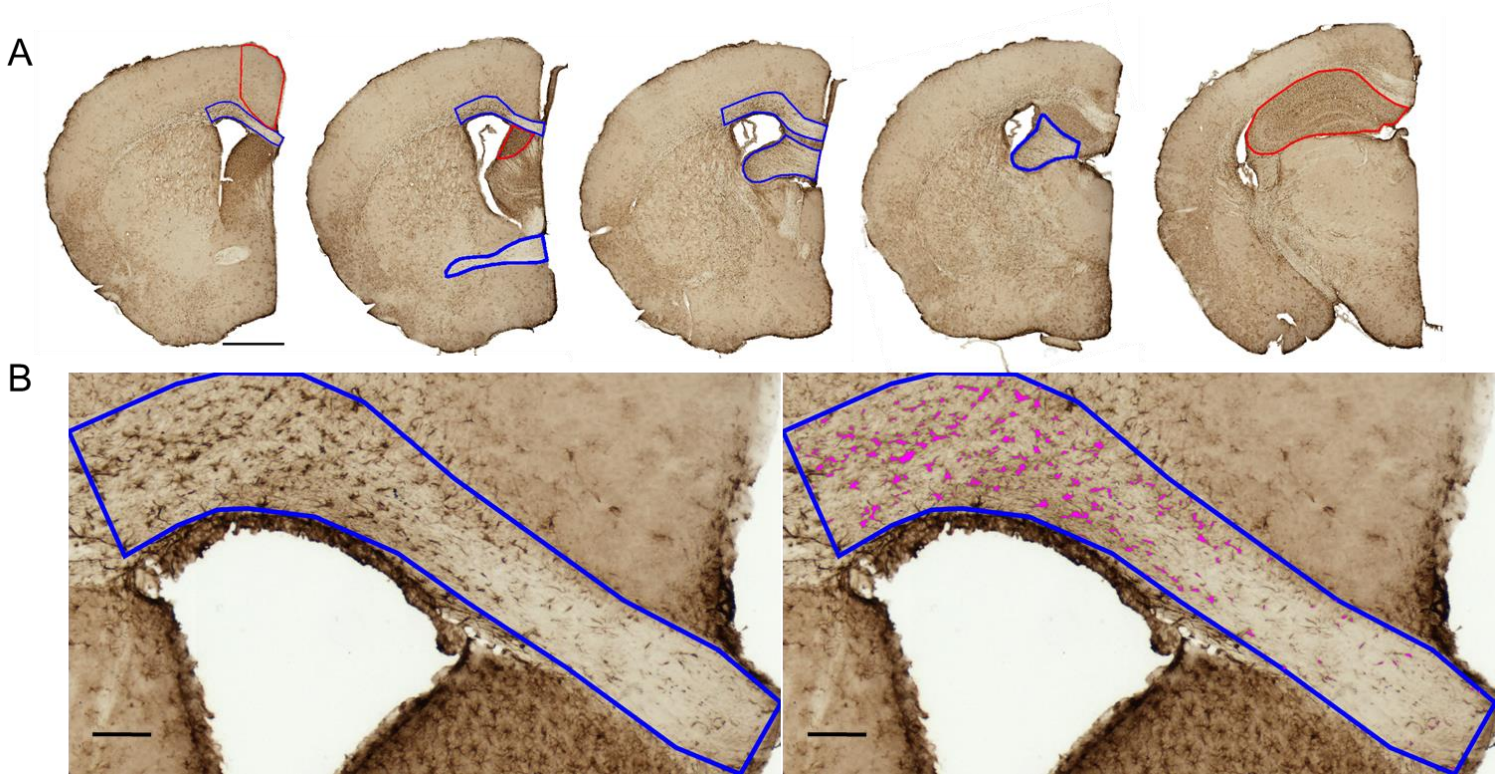

Supplemental Figure 3. Quantification of astrogliosis. A. Regions of interest were drawn to include the corpus callosum, cortical gray matter, lateral septal nucleus, anterior commissure, hippocampal commissure, fimbria, and hippocampus (red line = gray matter, blue line = white matter). Scale bar = 500 microns. **B.** Astrogliosis was quantified by thresholding images of the GFAP stained sections in FIJI, followed by size exclusion to remove edge artifacts and out of focus cell bodies. Scale bar = 100 microns.

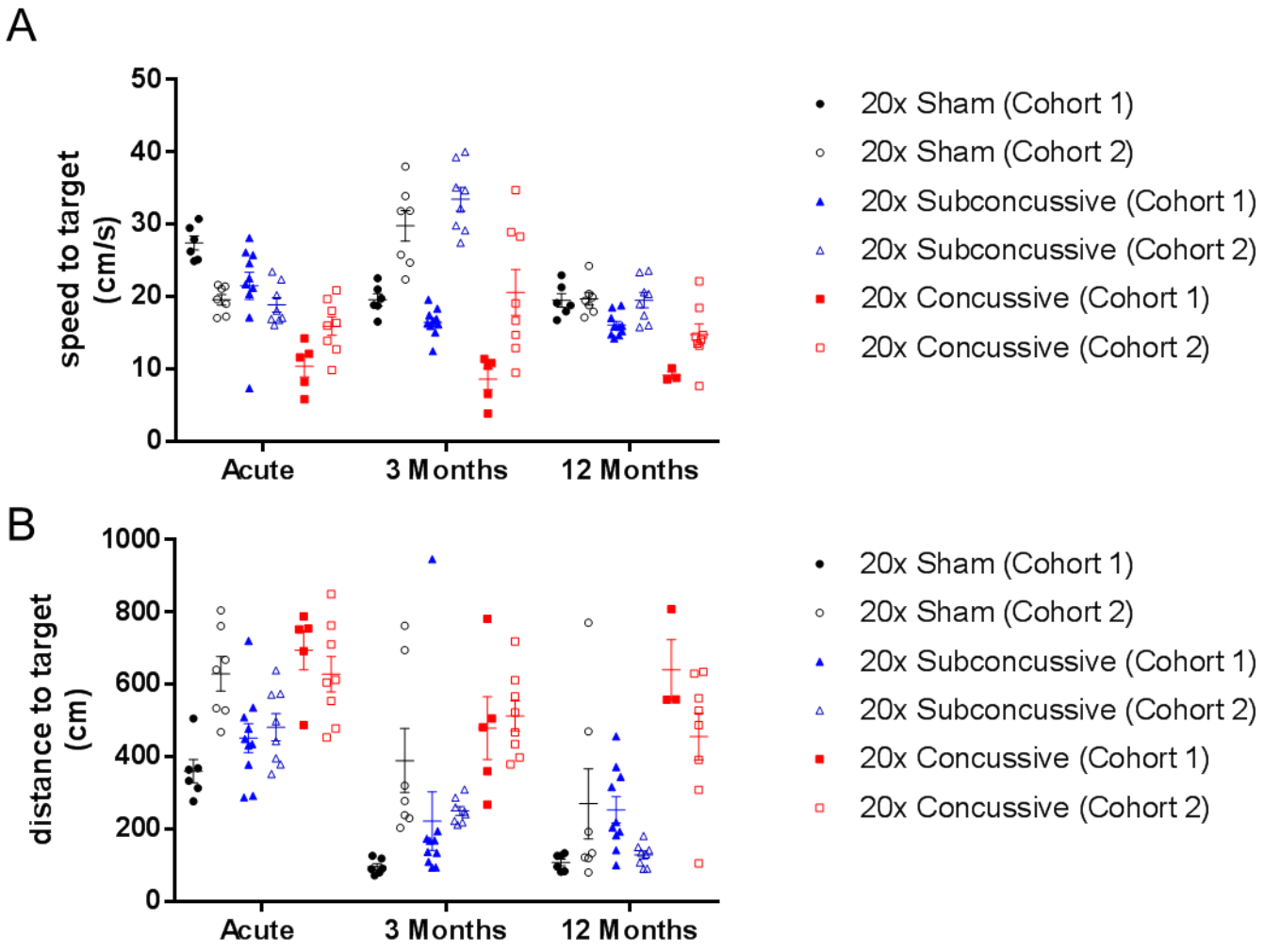

Supplemental Figure 4. Raw data of visible phase of Morris Water Maze. A. Swimming speeds during the visible phase of Morris Water Maze. Speeds represent the mean for each subject across the three days of visible platform for each test session. **B.** Distance to the target platform during the visible phase of Morris Water Maze. Distances represent the mean for each subject across the three days of visible platform for each test session.

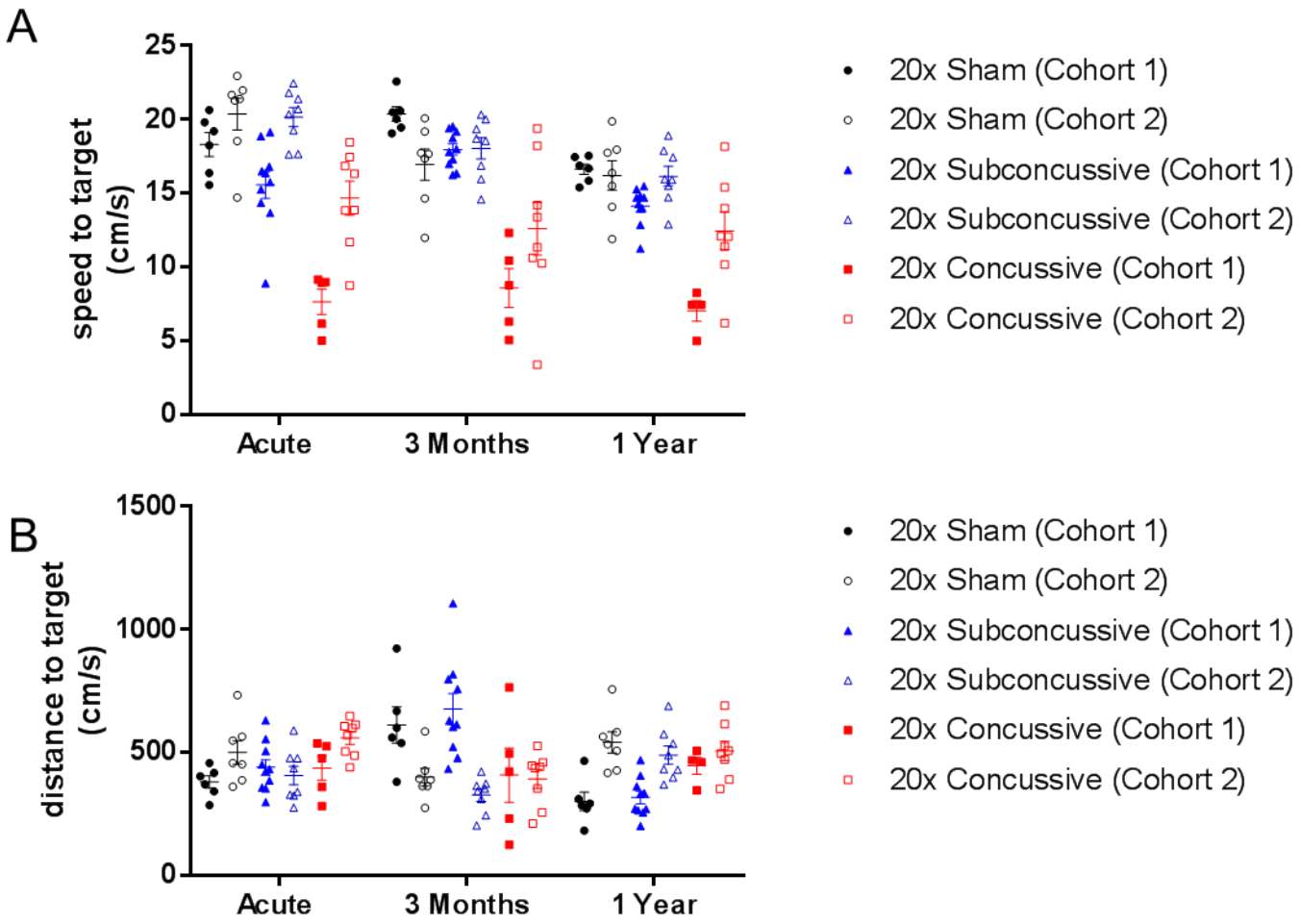

Supplemental Figure 5. Raw data of hidden phase of Morris Water Maze. A. Swimming speeds during the hidden phase of Morris Water. Speeds represent the mean for each subject across the four days of hidden platform for each test session **B.** Distance swum to platform during the hidden phase of Morris Water Maze. Distances represent the mean for each subject across the four days of hidden platform for each test session.

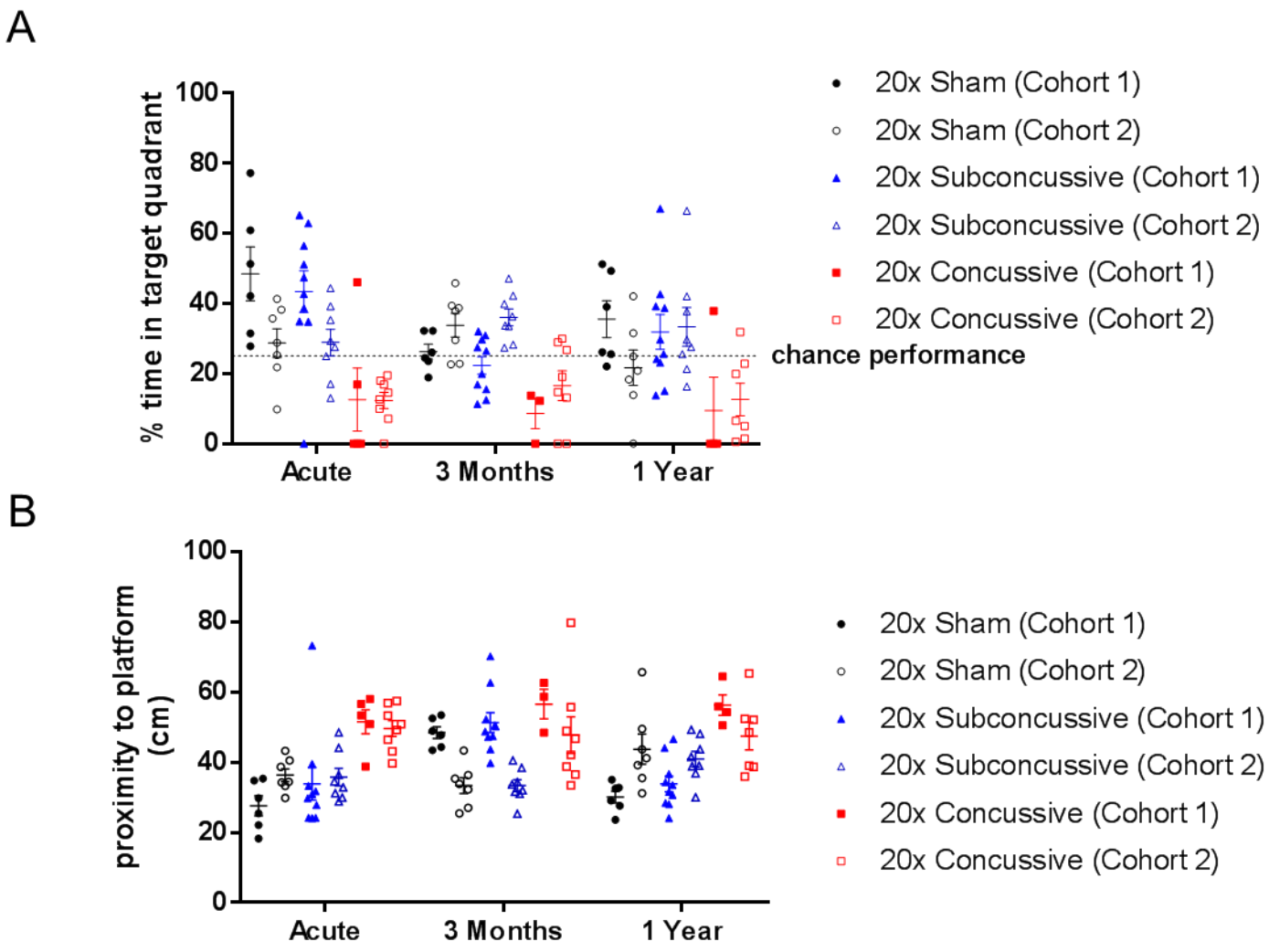

Supplemental Figure 6. Raw data of probe trial performance. A. Raw data of percent time spent in the target quadrant during probe trial. Dotted line indicates chance performance, where mice spending less than 25% of their time in the target quadrant show impaired memory. **B.** Raw data of the mean proximity to the location of where the platform had been placed during the preceding hidden platform phase. Increased proximity to platform indicates worse performance and impaired memory of the platform location.

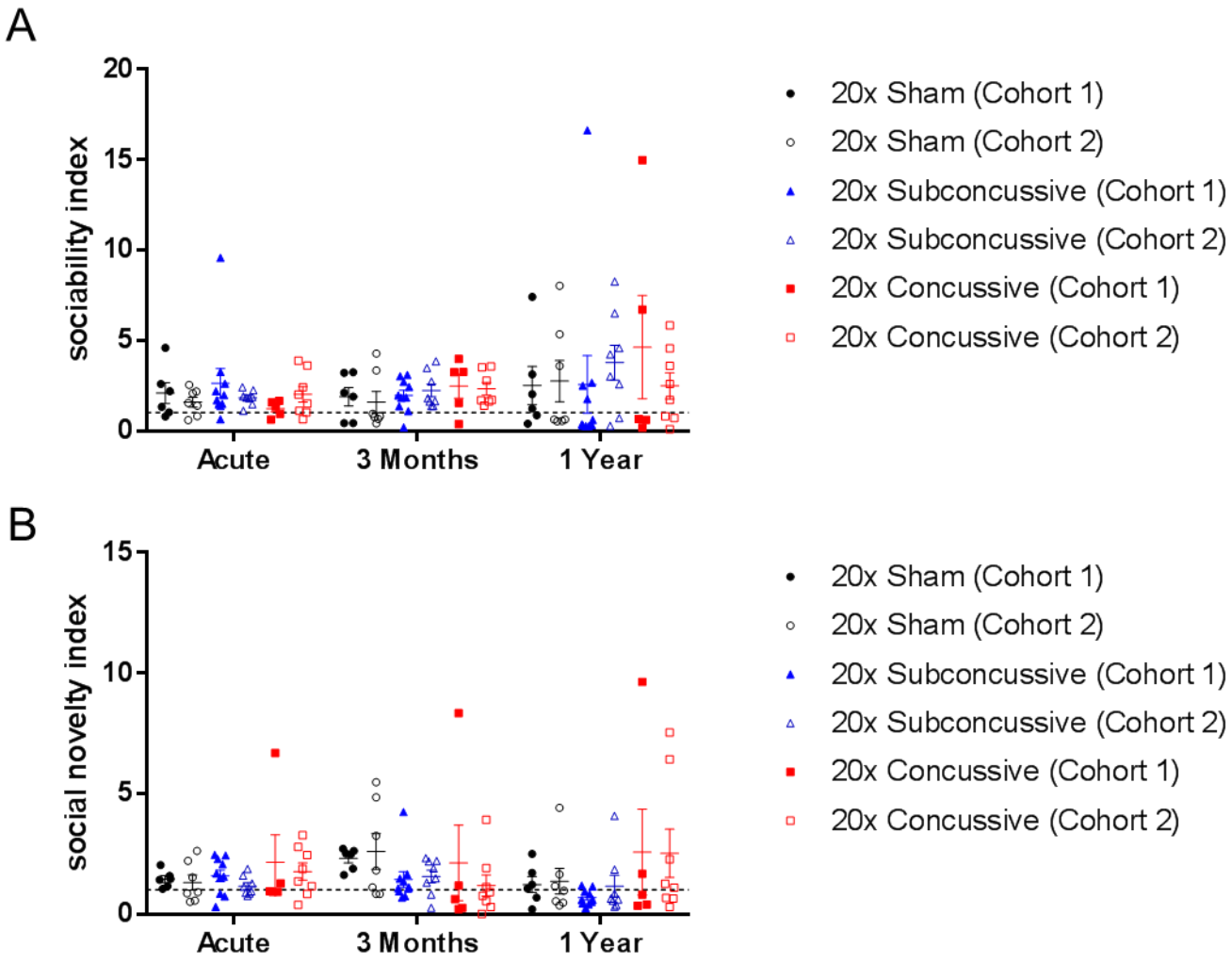

Supplemental Figure 7. Raw data of social interaction task. A. Raw data of sociability index during the three chamber social interaction test. Sociability index was calculated as the ratio of time interacting with the stimulus mouse to time spent with the novel object. The dotted line marks an index of one. Points above this line indicate that the animal preferred to interact with the stimulus mouse. **B.** Raw data of social novelty index during the three chamber social interaction test. Social novelty index was calculated as the ratio of time interacting with the novel mouse to time spent with the first stimulus mouse. The dotted line marks an index of one. Points above this line indicate that the animal preferred to interact with the novel mouse.

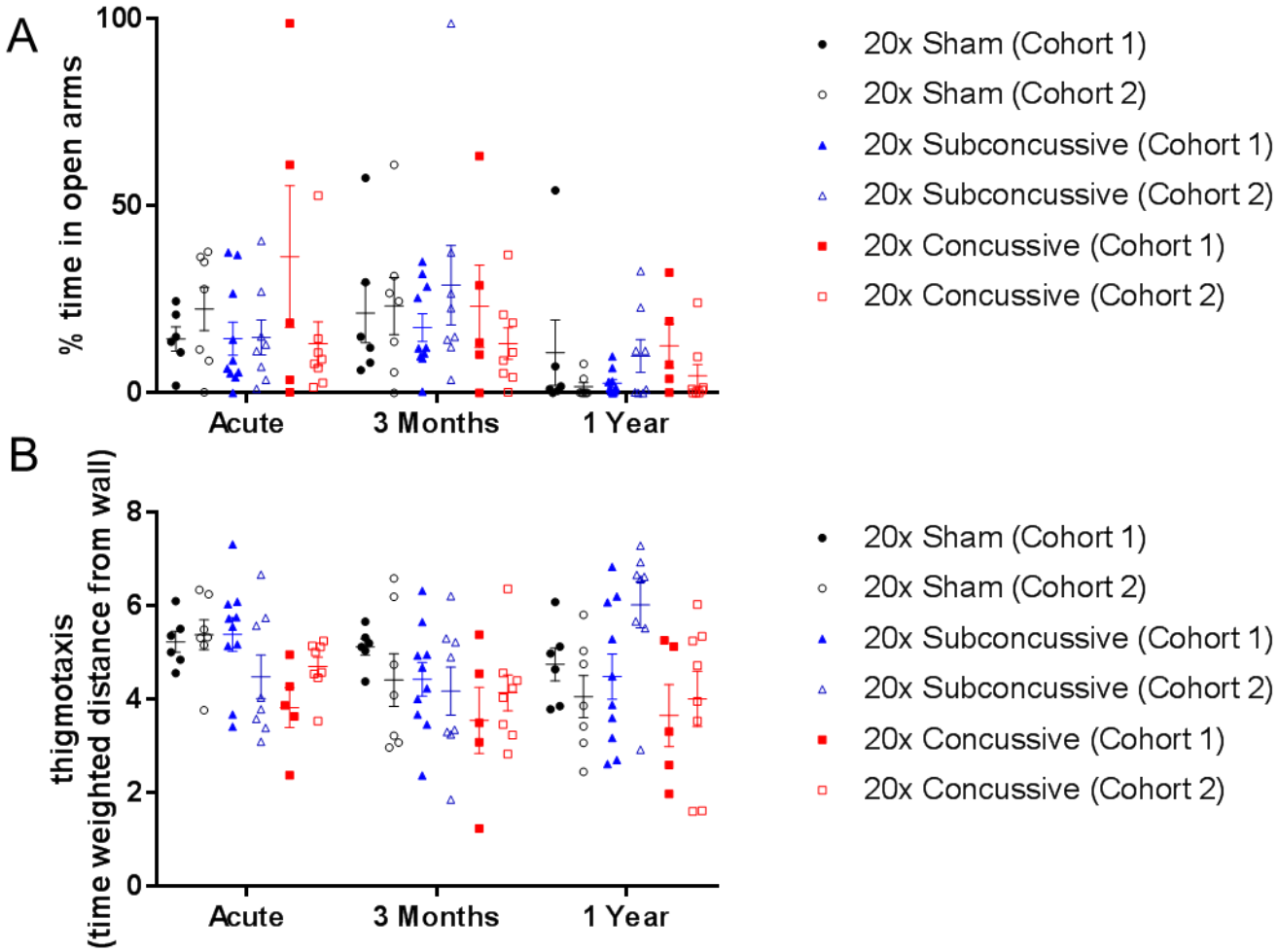

Supplemental Figure 8. Raw data of elevated plus maze and open field maze. A. Percent time spent in the open arms of the elevated plus maze. **B.** Raw data of open field maze thigmotaxis, measured as the time weighted distance from the maze wall.

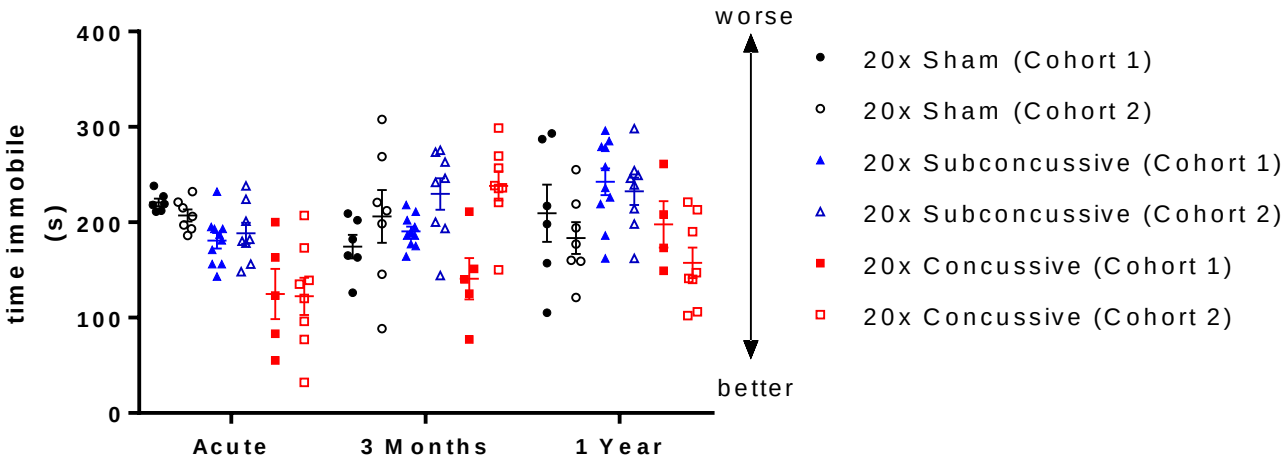

Supplemental Figure 9. Raw data of tail suspension test. Raw data of time immobile during a six minute tail suspension test was measured for each animal during each test session.

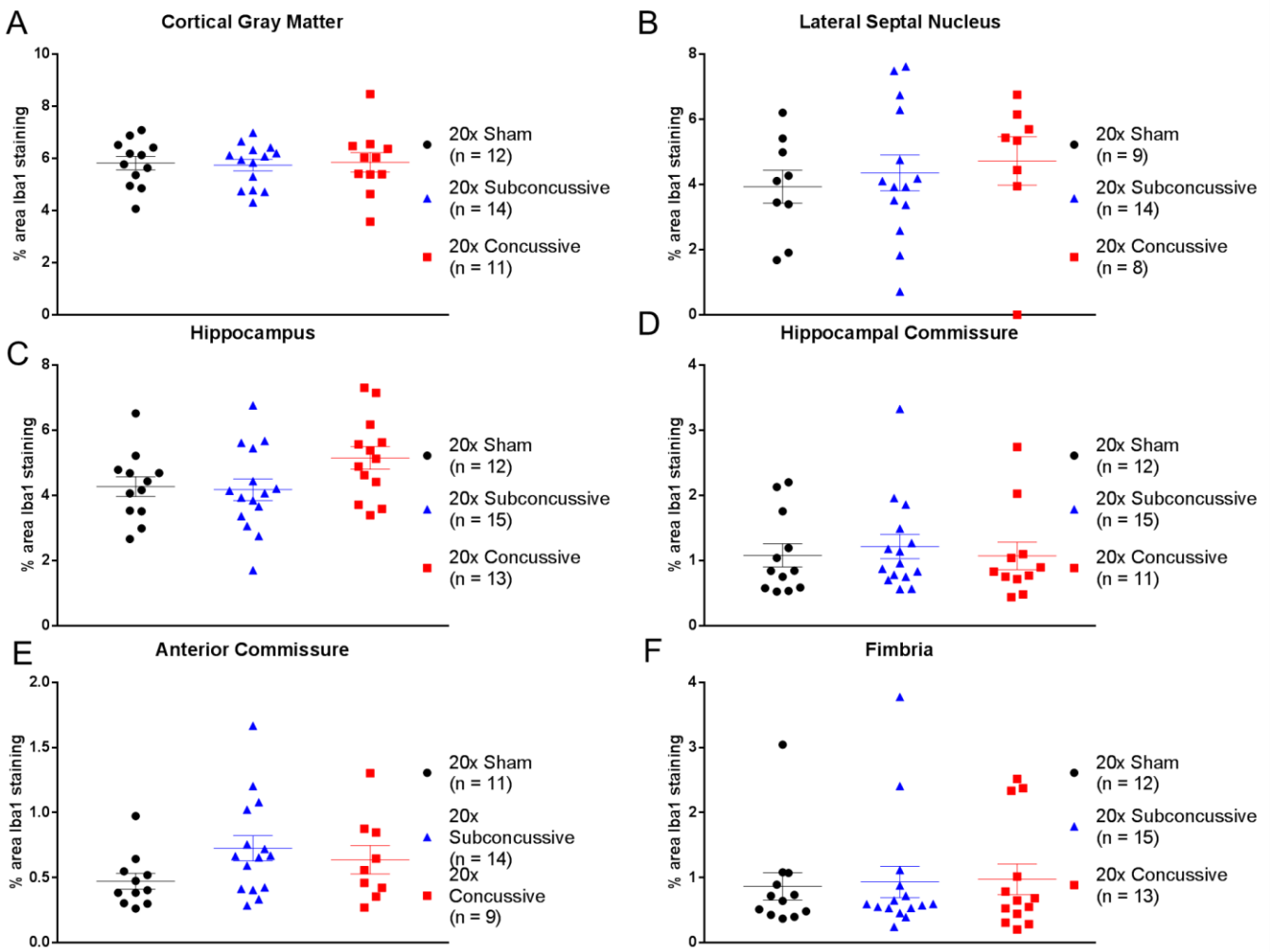

Supplemental Figure 10. Changes in gray and white matter microgliosis following repetitive head injuries. A. Percent area of thresholded Iba1 staining was measured in cortical gray matter. There was no effect of injury on staining. **B.** No differences in microgliosis measured by Iba1 staining were evident in the lateral septal nucleus. **C.** There were no injury related differences on microgliosis in the hippocampus. **D.** No injury related differences in Iba1 staining were detected in the hippocampal commissure. **E.** There was no effect of injury on percent area of Iba1 staining in the anterior commissure. **F.** There were no differences in microgliosis in the fimbria between injury groups.

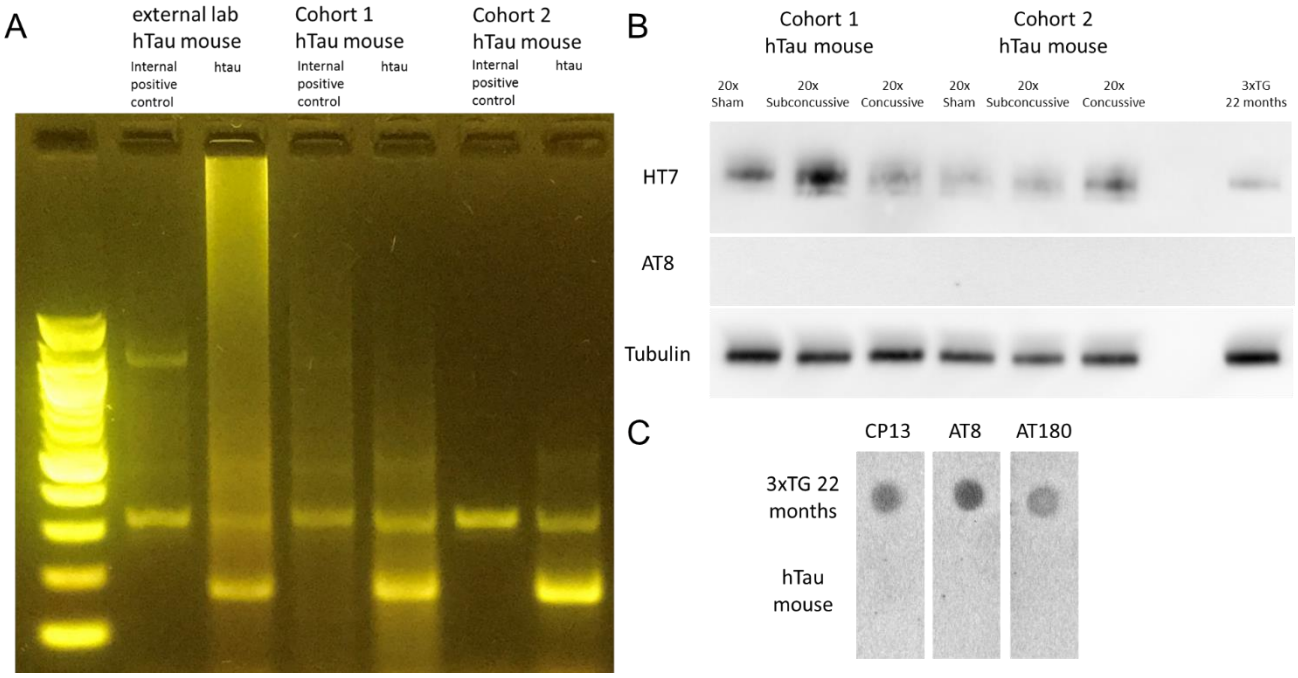

Supplemental Figure 11. PCR and Western blotting in hTau mice. A. PCR was performed by DNA extraction from fresh-frozen brain tissue of one hTau mouse randomly selected from each cohort of animals purchased from Jackson Laboratory. As a positive control, tail DNA from an hTau mouse was obtained from an independent investigator. The animals from each cohort tested positive for the hTau transgene. **B.** Western blotting successfully detected the presence of total human tau (HT7) in hippocampal homogenates of hTau animals from both cohorts and all three injury groups. Hippocampal tissue from a 22 month old 3xTG animal was used as a positive control. Surprisingly, all samples including the positive control showed no indication of phosphorylated tau, indicating low levels of phosphorylated tau in homogenized tissue lysates. **C.** A dot blot assay run on protein lysate from both 3xTG and hTau hippocampal tissue showed strong positive signal for CP13 (pSer202), AT8 (pSer202/pTher205), and AT180 (pThr231) in 3xTG but not hTau mice, indicating low or minimal starting levels of phosphorylated tau.

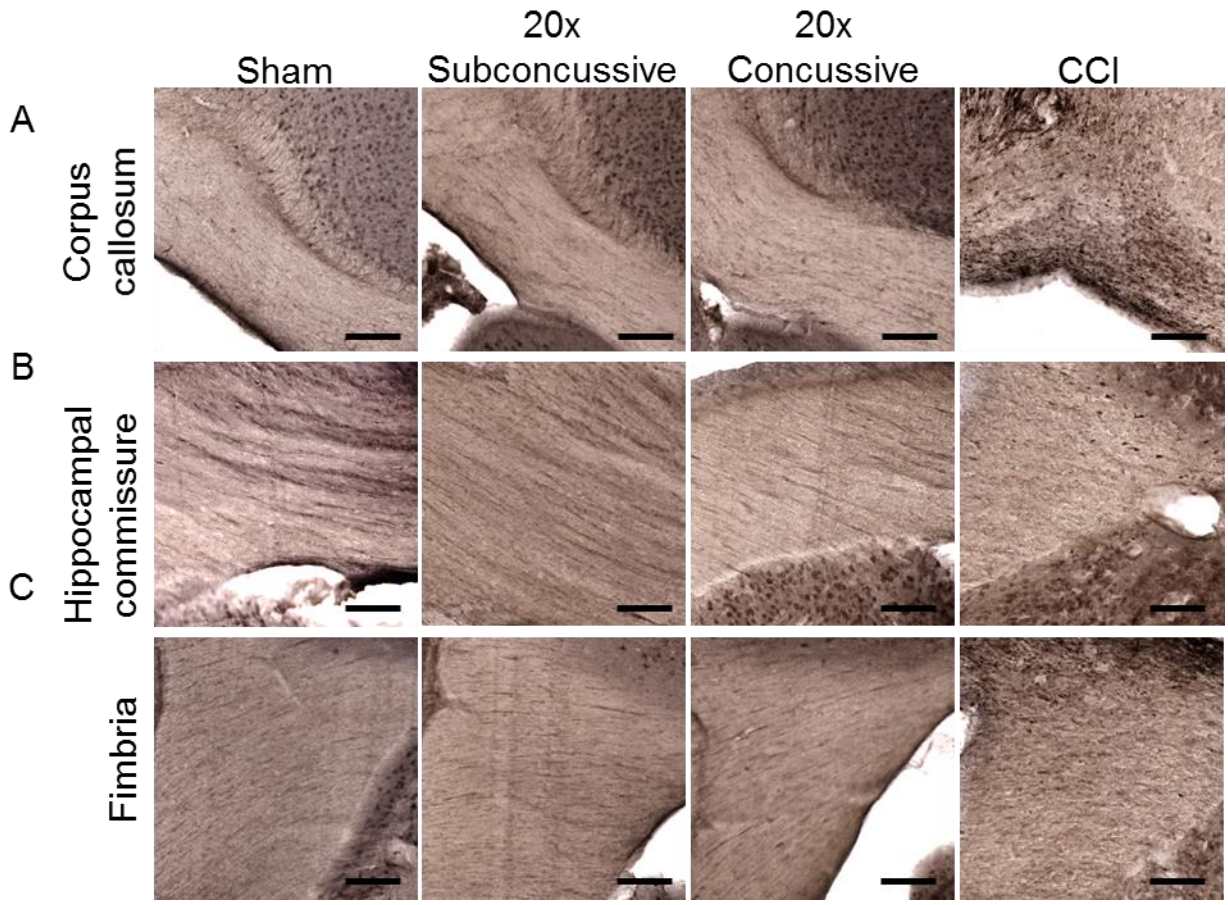

Supplemental Figure 12. APP staining one year following repetitive head injury. A. APP staining showed no differences of staining in the corpus callosum of 20x sham, subconcussive or concussive hTau animals. The positive control controlled cortical impact (CCI) tissue shows positive staining in the pericontusional region. **B.** No APP irregularities were observed between the injury groups in the hippocampal commissure. **C.** APP staining revealed no differences between sham, subconcussive and concussive injury groups. Scale bar = 100 microns.

Authors	Animal type	Age at time of injury	Injury model	Injury number	Inter-injury interval	Acute behavioral outcomes	Acute pathology	Chronic behavioral outcomes	Chronic pathology
Kanayama et al 1996[1]	Rat	N/A	FPI	7	24 hours	1 week: impaired habituation to novel environment	1 week: Accumulation of MAP2 and NFH spreading to the contralateral cortex and hippocampus. pTau immunoreactivity in cortical neurons	N/A	N/A
Creeley et al 2004[2]	C57BL/6	7-8 weeks	Weight drop	3	24 hours	Impaired spatial learning during MWM	Silver staining abnormalities in olfactory and optic tracts	N/A	N/A
Shitaka et al 2011[3]	C57BL/6	2-3 months	Closed head impact	2	24 hours	MWM deficits	Abnormal APP swellings, argyrophylic abnormalities	7 weeks: MWM deficits	Persistent microglial activation, white matter silver staining
Ojo et al 2013[4]	hTau mice	18 months	Closed head CCI	5	48 hours	N/A	Increased ptau immunoreactivity no perivascular or astroglial tau. Increased microglial and astrocytic reactivity	N/A	N/A
Mannix et el 2013[5]	C57BL/6	2-3 months	Weight drop	7	24 hours	Impaired balance and MWM deficits	N/A	12 months: Impaired balance and MWM deficits	6 months: elevated microgliosis and astrogliosis
Petraglia et al 2014a/2014b[6, 7]	C57BL/6	3 months	Closed head CCI with acceleration/ deceleration (no anesthesia)	42	2 hours	Elevated NSS, increased anxiety like behavior, MWM deficits, sleep disturbances, depressive behavior	Reactive astrocytosis elevated ptau immunoreactivity	Increased risk taking behavior at 6 months persistent MWM deficits	6 months; astrogliosis and microgliosis, increased ptau immunoreactivity
Luo et al 2014[8]	C57BL/6	2-3 months	Closed head CCI	3	24 hours	Spatial learning and memory deficits	N/A	6 months post injury; spatial learning and memory deficits	6 months post injury; increased astrogliosis, increased ptau immunoreactivity
Turner et al 2015[9]	Sprague-Dawley rats	N/A	Blast injury	6	48 hours	Increased open arm time in EPM, MWM deficits	Increased ptau immunoreactivity	N/A	N/A
Bajwa et al 2016[10]	C57BL/6	3 months	Unrestrained closed head CCI	2	72 hours	No differences	N/A	90 days post injury; increased depressive like behavior Reduced social activity	N/A

Ojo et al 2016[11]	hTau mice	3 months	Closed head CCI	24 or 32	72 or 96 hours	N/A	N/A	6 months post injury; impaired MWM performance, increased risk taking behavior	Increased total tau levels, mild increase in ptau.
Chen et al 2017[12]	C57BL/6	12 weeks	0.5J CHIMERA	3	24 hours	Motor deficits, MWM deficits	APP deposition, reduced by 1 month	6 months post injury; impaired MWM deficits	Increased GFAP, Iba1 levels

Supplemental Table 1. Preclinical animal models of repetitive traumatic brain injury. Multiple groups have implemented repetitive head injury paradigms in rodent models (mouse and rat) in an attempt to study chronic phosphorylated tau pathology commonly found in human patients diagnosed with chronic traumatic encephalopathy.

Dataset	Normally distributed? (Shapiro Wilk ($p < 0.05$)	Transformation applied	Effect of Cohort
Three chamber social interaction: sociability index	No	Rank (no ties)	No
Three chamber social interaction: social novelty index	No	Rank (no ties)	No
Open field maze: thigmotaxis	Yes	N/A	No
Elevated plus maze: % time in open arms	No	Rank (no ties)	No
Morris Water Maze visible platform: speed to target	No	Averaged across test session	No
Morris Water Maze visible platform: distance to target	No	Averaged across test session	No
Morris Water Maze hidden platform: speed to target	No	Square root	No
Morris Water Maze hidden platform: speed to target	No	Rank transformed averaged across test session (no ties)	No
Morris Water Maze probe trial: proximity to platform	No	Inverse (1/x)	No
Morris Water Maze probe trial: % time in target quadrant	No	Rank	No
Astrogliosis: % area GFAP staining	Yes	N/A	No
White matter integrity: power coherence	Yes	N/A	No
Microgliosis: % area Iba1 staining	Yes	N/A	No

Supplemental Table 2. List of transformations applied for statistical analysis of data. Datasets where the residuals were not normally distributed (Shapiro Wilkes, $p<0.05$), were transformed so that residuals would be normally distributed. A two way (repeated measures for behavioral data) ANOVA was then used to test for effects of injury and cohort. Once transformed, there was no effect of cohort, allowing us to collapse the datasets for the two cohorts. Post-hoc Tukey testing was then used to test for significant effects of repetitive subconcussive and concussive injury.

Behavioral/Histological Test	$F_{(df,error)}$	Effect Size (η^2_p)
Latency righting reflex	$F_{(2,44)} = 11.8092$	0.349
MWM visible platform: swim speed	$F_{(2,36)} = 29.9335$	0.624
MWM visible platform: swimming distance	$F_{(2,36)} = 25.642$	0.588
MWM hidden platform: swim speed	$F_{(2,36)} = 36.5009$	0.663
MWM hidden platform: swimming distance	$F_{(2,36)} = 6.272$	0.564
MWM probe trial: proximity to platform	$F_{(2,36)} = 23.173$ (Injury) $F_{(2,70)} = 6.9935$ (Time)	0.570 (Injury) 0.167 (Time)
MWM probe trial: % time in target quadrant	$F_{(2,36)} = 22.851$	0.566
Three chamber social interaction: sociability	$F_{(2,37)} = 0.300$	0.0159
Three chamber social interaction: social novelty	$F_{(2,37)} = 2.729$	.0860
Open field maze: thigmotaxis	$F_{(2,37)} = 3.610$	0.0243
Elevated plus maze: % time in open arms	$F_{(2,37)} = 0.195$	0.00102
Tail suspension: time immobile	$F_{(2,37)} = 12.954$	0.412
Astrogliosis: % area GFAP staining cortical gray matter	$F_{(2,31)} = 135.77$	0.125
Astrogliosis: % area GFAP staining lateral septal nucleus	$F_{(2,21)} = 62.55$	0.368
Astrogliosis: % area GFAP staining hippocampus	$F_{(2,30)} = 474.92$	0.00868
Astrogliosis: % area GFAP staining corpus callosum	$F_{(2,29)} = 349.54$	0.0156
Astrogliosis: % area GFAP staining anterior commissure	$F_{(2,27)} = 17.53$	0.0138
Astrogliosis: % area GFAP staining hippocampal commissure	$F_{(2,25)} = 116.08$	0.0126
Astrogliosis: % area GFAP staining fimbria	$F_{(2,28)} = 136.95$	0.0778
White matter integrity: power coherence corpus callosum	$F_{(2,37)} = 28.048$	0.644
White matter integrity: power coherence anterior commissure	$F_{(2,25)} = 183.19$	0.144
White matter integrity: power coherence hippocampal commissure	$F_{(2,37)} = 34.015$	0.687
White matter integrity: power coherence fimbria	$F_{(2,37)} = 17.262$	0.527
Microgliosis: % area Iba1 staining cortical gray matter	$F_{(2,34)} = 0.038$	0.0022
Microgliosis: % area Iba1 staining lateral septal nucleus	$F_{(2,28)} = 0.354$	0.0257
Microgliosis: % area Iba1 staining hippocampus	$F_{(2,37)} = 2.635$	0.125
Microgliosis: % area Iba1 staining corpus callosum	$F_{(2,34)} = 7.984$	0.320
Microgliosis: % area Iba1 staining anterior commissure	$F_{(2,32)} = 2.019$	0.112
Microgliosis: % area Iba1 staining hippocampal commissure	$F_{(2,35)} = 0.338$	0.190
Microgliosis: % area Iba1 staining fimbria	$F_{(2,37)} = 0.538$	0.0029

Supplemental Table 3. List of effect sizes for ANOVAs. The F distribution, described by the degrees of freedom and error, along with effect sizes (η^2_p) were calculated for each behavioral and histological parameter assessed.

SUPPLEMENTARY REFERENCES

1. Kanayama, G., Takeda, M., Niigawa, H., Ikura, Y., Tamii, H., Taniguchi, N., Kudo, T., Miyamae, Y., Morihara, T. and Nishimura, T. (1996). The effects of repetitive mild brain injury on cytoskeletal protein and behavior. Methods Find Exp Clin Pharmacol 18, 105-115.
2. Creeley, C.E., Wozniak, D.F., Bayly, P.V., Olney, J.W. and Lewis, L.M. (2004). Multiple episodes of mild traumatic brain injury result in impaired cognitive performance in mice. Acad Emerg Med 11, 809-819.
3. Shitaka, Y., Tran, H.T., Bennett, R.E., Sanchez, L., Levy, M.A., Dikranian, K. and Brody, D.L. (2011). Repetitive closed-skull traumatic brain injury in mice causes persistent multifocal axonal injury and microglial reactivity. J Neuropathol Exp Neurol 70, 551-567.
4. Ojo, J.O., Mouzon, B., Greenberg, M.B., Bachmeier, C., Mullan, M. and Crawford, F. (2013). Repetitive mild traumatic brain injury augments tau pathology and glial activation in aged hTau mice. J Neuropathol Exp Neurol 72, 137-151.
5. Mannix, R., Meehan, W.P., Mandeville, J., Grant, P.E., Gray, T., Berglass, J., Zhang, J., Bryant, J., Rezaie, S., Chung, J.Y., Peters, N.V., Lee, C., Tien, L.W., Kaplan, D.L., Feany, M. and Whalen, M. (2013). Clinical correlates in an experimental model of repetitive mild brain injury. Ann Neurol 74, 65-75.
6. Petraglia, A.L., Plog, B.A., Dayawansa, S., Dashnaw, M.L., Czerniecka, K., Walker, C.T., Chen, M., Hyrien, O., Iliff, J.J., Deane, R., Huang, J.H. and Nedergaard, M. (2014). The pathophysiology underlying repetitive mild traumatic brain injury in a novel mouse model of chronic traumatic encephalopathy. Surg Neurol Int 5, 184.
7. Petraglia, A.L., Plog, B.A., Dayawansa, S., Chen, M., Dashnaw, M.L., Czerniecka, K., Walker, C.T., Viterise, T., Hyrien, O., Iliff, J.J., Deane, R., Nedergaard, M. and Huang, J.H. (2014). The spectrum of neurobehavioral sequelae after repetitive mild traumatic brain injury: a novel mouse model of chronic traumatic encephalopathy. J Neurotrauma 31, 1211-1224.
8. Luo, J., Nguyen, A., Villeda, S., Zhang, H., Ding, Z., Lindsey, D., Bieri, G., Castellano, J.M., Beaupre, G.S. and Wyss-Coray, T. (2014). Long-term cognitive impairments and pathological alterations in a mouse model of repetitive mild traumatic brain injury. Front Neurol 5, 12.
9. Turner, R.C., Lucke-Wold, B.P., Logsdon, A.F., Robson, M.J., Dashnaw, M.L., Huang, J.H., Smith, K.E., Huber, J.D., Rosen, C.L. and Petraglia, A.L. (2015). The Quest to Model Chronic Traumatic Encephalopathy: A Multiple Model and Injury Paradigm Experience. Front Neurol 6, 222.
10. Bajwa, N.M., Halavi, S., Hamer, M., Semple, B.D., Noble-Haeusslein, L.J., Baghchechi, M., Hiroto, A., Hartman, R.E. and Obenaus, A. (2016). Mild Concussion, but Not Moderate Traumatic Brain Injury, Is Associated with Long-Term Depression-Like Phenotype in Mice. PLoS One 11, e0146886.
11. Ojo, J.O., Mouzon, B., Algamal, M., Leary, P., Lynch, C., Abdullah, L., Evans, J., Mullan, M., Bachmeier, C., Stewart, W. and Crawford, F. (2016). Chronic Repetitive Mild Traumatic Brain Injury Results in Reduced Cerebral Blood Flow, Axonal Injury, Gliosis, and Increased T-Tau and Tau Oligomers. J Neuropathol Exp Neurol 75, 636-655.
12. Chen, H., Desai, A. and Kim, H.Y. (2017). Repetitive Closed-Head Impact Model of Engineered Rotational Acceleration Induces Long-Term Cognitive Impairments with Persistent Astrogliosis and Microgliosis in Mice. J Neurotrauma 34, 2291-2302.